SUPPORTING INFORMATION

Demonstration of efficient electrochemical biogas reforming in solid oxide electrolyser with titanate cathode

Qingqing Qin,[a] Kui Xie,[a,b] * Haoshan Wei,[a] Wentao Qi,[a] Jiewu Cui, [a] Yucheng Wu[a,b] *

[a]Department of Energy Materials, School of Materials Science and Engineering, Hefei University of Technology, No.193 Tunxi Road, Hefei, Anhui 230009, China

[b]Key Laboratory of Advanced Functional Materials and Devices, School of Materials Science and Engineering, Hefei University of Technology, No.193 Tunxi Road, Hefei, Anhui 230009, China

*Corresponding: xiekui@hfut.edu.cn

Captions

Figure S1: Schematic of the *in-situ* electrochemical electrochemical biogas reforming in an oxide-ion-conducting solid oxide electrolyzer with the configuration $(La_{0.8}Sr_{0.2})_{0.95}MnO_{3-\delta}$/YSZ/$La_{0.2}Sr_{0.8}TiO_{3+\delta}$.

Figure S2: The conductivity of LSTO: (a) reduced LSTO in 5% H_2/Ar; (b) in different oxygen partial pressure at 800 °C.

Figure S3: XPS results of La (a) in the oxidized LSTO sample; (b) in the reduced LSTO samples.

Figure S4: The R_p of the symmetric cells with the configuration LSTO-SDC/YSZ/LSM-SDC and iron-loaded LSTO-SDC/YSZ/LSM-SDC tested under different hydrogen partial.

Figure S5: SEM cathode surface of the composite cathode after short-term operation of the electrochemical biogas reforming with LSTO-SDC cathode.

Figure S6: The XRD pattern of $Ce_{0.8}Sm_{0.2}O_{2-\delta}$ powder by a heat treatment at 800 °C for 3 h in air.

Figure S7: R_p of the electrolysis cells with cathodes based on LSTO-SDC and iron-loaded LSTO-SDC in 20%CH_4/20%CO_2/60%Ar under different applied potentials at 800 °C.

Figure S8: The conversion of CO_2 and CH_4 : (a) based on LSTO and (b2) based on iron-loaded LSTO in the flow of 20%CH_4/20%CO_2/60%Ar at 800 °C.

Figure S9: (a) The production of H_2; (b) The production of CO with LSTO and iron-loaded LSTO in the flow of 20%CH_4/20%CO_2/60%Ar at 800 °C.

Figure S10: XRD pattern of Fe_2O_3 powder treated at different temperatures from 400-800 °C.

Figure S11: particle size of Fe_2O_3 powder treated at different temperatures from 400-800 °C.

Figure S1:

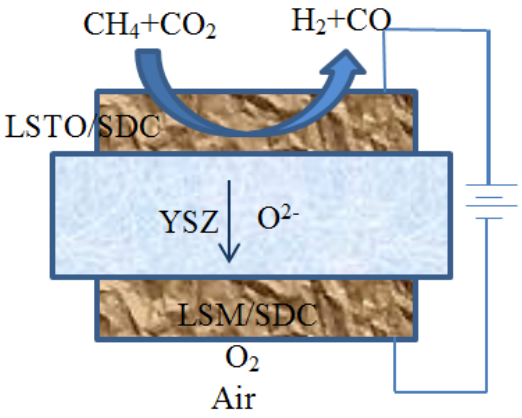

Figure S2:

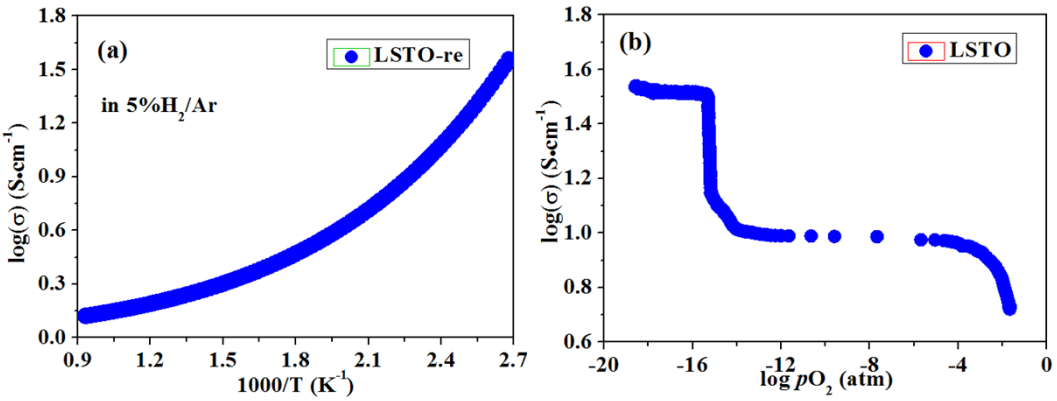

Figure S3

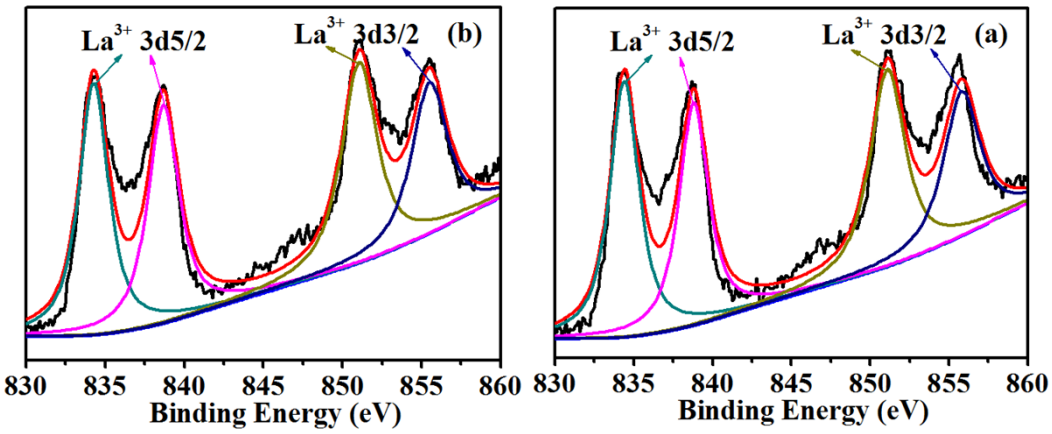
La3+ 3d5/2
La3+ 3d3/2
(b)
La3+ 3d5/2
La3+ 3d3/2
(a)
830 835 840 845 850 855 860
Binding Energy (eV)
830 835 840 845 850 855 860
Binding Energy (eV)

Figure S4:

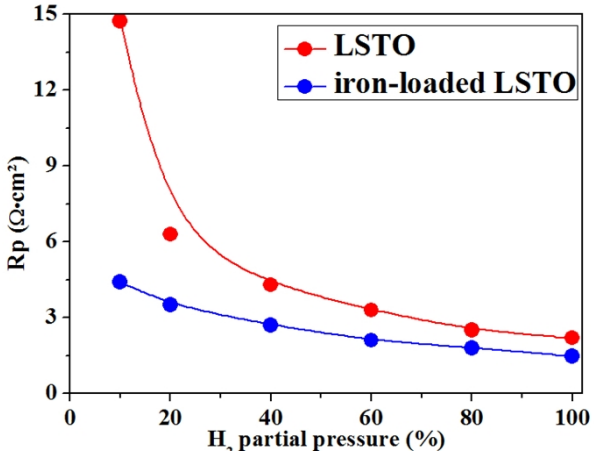
LSTO
iron-loaded LSTO
Rp (Ω·cm²)
H₂ partial pressure (%)
0
3
6
9
12
15
0
20
40
60
80
100

Figure S5:

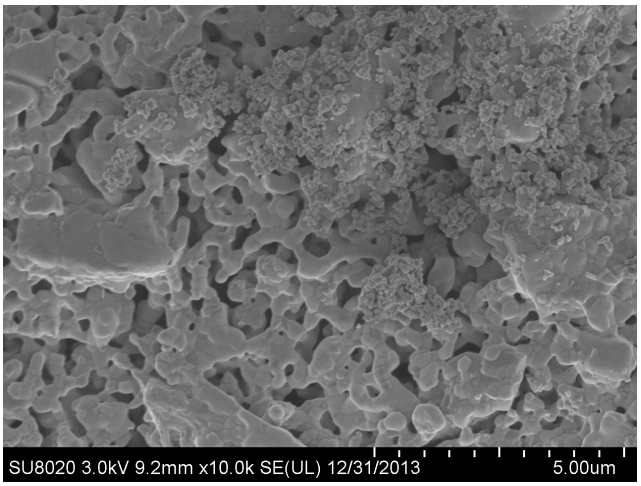

Figure S6:

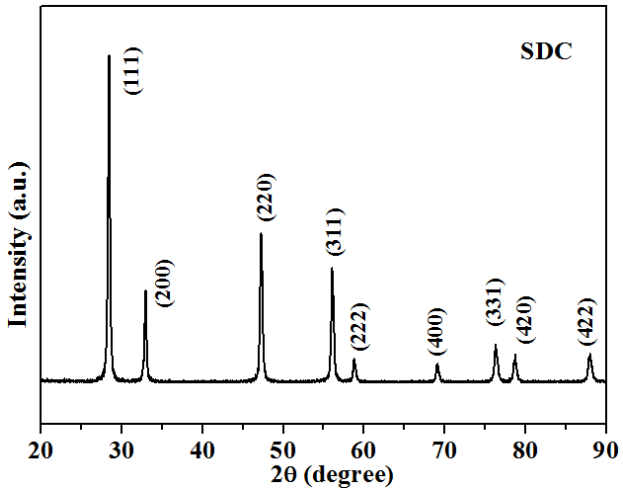
SDC
(111)
(200)
(220)
(311)
(222)
(400)
(331)
(420)
(422)
Intensity (a.u.)
20
30
40
50
60
70
80
90
2θ (degree)

Figure S7:

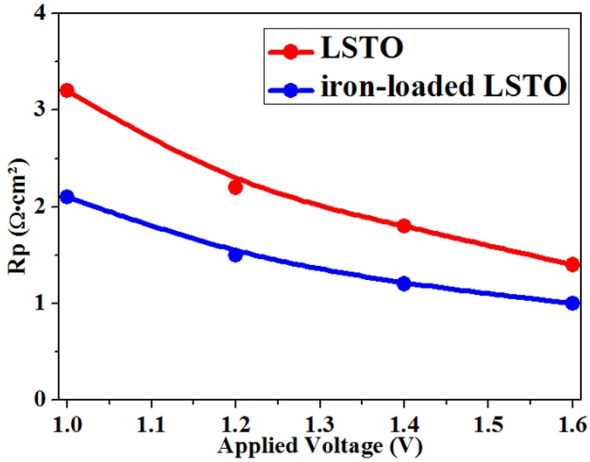
LSTO
iron-loaded LSTO
Rp (Ω·cm²)
Applied Voltage (V)
0
1
2
3
4
1.0
1.1
1.2
1.3
1.4
1.5
1.6

Figure S8:

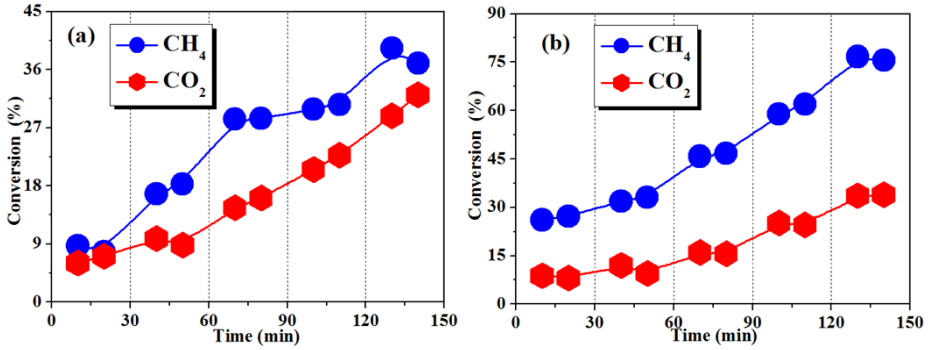
(a)
CH4
CO2
Conversion (%)
Time (min)
0
9
18
27
36
45
0
30
60
90
120
150
(b)
CH4
CO2
Conversion (%)
Time (min)
0
15
30
45
60
75
90
0
30
60
90
120
150

Figure S9:

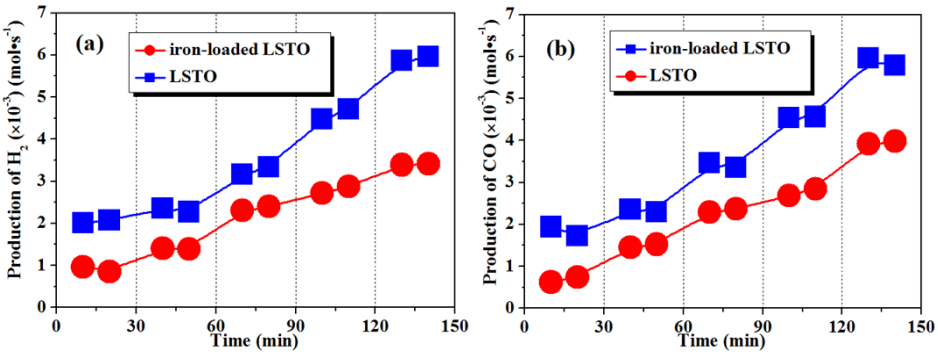
(a)
iron-loaded LSTO
LSTO
Production of H_2 ($\times 10^{-3}$) (mols^{-1})
Time (min)
(b)
iron-loaded LSTO
LSTO
Production of CO ($\times 10^{-3}$) (mols^{-1})
Time (min)

Figure S10:

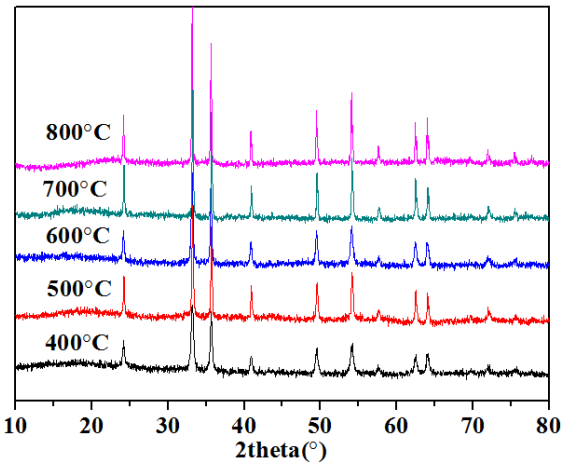

Figure S11:

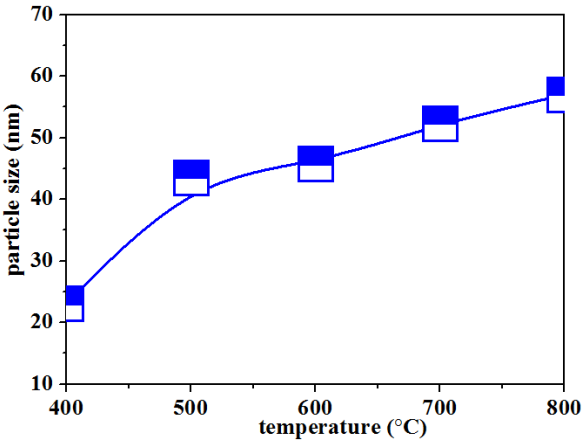
70
60
50
40
30
20
10
particle size (nm)
400
500
600
700
800
temperature (°C)